Original Article

Assessment of phytoplankton group composition in the Golden Horn Estuary (Sea of Marmara, Turkey) determined with pigments measured by HPLC-CHEMTAX analyses and microscopy

Fuat Dursun [ID], Seyfettin Tas [ID] and Dilek Ediger

Institute of Marine Sciences and Management, Istanbul University, 34134, Vefa, Fatih, Istanbul, Turkey

Abstract

Phtytoplankton group composition determined by microscopy was compared with high performance liquid chromatography (HPLC) derived from pigment signatures in surface water samples taken bi-weekly and monthly between October 2018 and September 2019 in the Golden Horn Estuary (Sea of Marmara). A total of 80 eukaryotic phytoplankton taxa belonging to eight algal classes were identified in surface water during the study period. Forty-three taxa (54%) were diatoms, 29 taxa (36%) were dinoflagellates and eight taxa (10%) were other phytoflagellates. The average contribution of diatoms to total phytoplankton abundance decreased considerably (41 to 25%), while the average contribution of dinoflagellates and other phytoflagellates increased markedly (59 to 75%) from the lower to the middle estuary. Chlorophyll-*a* and seven other group-specific pigments, including fucoxanthin, peridinin, chlorophyll-$c_1 + c_2$, alloxanthin, 19′-hexanoyloxyfucoxanthin, 19′-butanoyloxyfucoxanthin and divinyl chlorophyll-*a* were identified in the study area. The relative contribution of the major phytoplankton groups to chlorophyll-*a* was estimated on three different initial ratio matrices by CHEMTAX. The results obtained were compared with those from microscopic examination. It was concluded that the CHEMTAX method was not accurate enough to characterize the phytoplankton community in the Golden Horn Estuary ecosystem and microscopic analysis was essential to determine the major contributing species to chlorophyll-*a*.

Introduction

Phytoplankton is generally constituted of complex communities and their diversity and dynamics are highly variable. Information about the combined effects of various environmental variables is necessary in food chain studies and ecosystem modelling as well as for explaining eutrophication and harmful algal bloom events (Wänstrand & Snoeijs, 2006). Thus, distribution of phytoplankton species provides crucial data for environmental monitoring studies. As these species can change in a very short time, regular investigation of phytoplankton composition requires substantial resources for sampling and skilled staff for microscopy (Hillebrand *et al.*, 1999).

The identification of phytoplankton through microscopic analysis is time-consuming and needs a high level of taxonomic expertise. There is also the risk of missing smaller phytoplankton groups (like picoplankton, <2 μm in size) in traditional microscopic analysis (Naik *et al.*, 2011). An alternative or supplementary method for monitoring and identifying phytoplankton community structures is to determine their pigment signatures by using high-performance liquid chromatography (HPLC) (Wright & Jeffrey, 2006). This technique is faster and more reproducible than microscopy and independent of subjective consideration (Wänstrand & Snoeijs, 2006). Moreover, this technique can be more sensitive for identifying pico- and nanoplankton or species broken by sample fixation, which can be difficult to identify with microscopic analysis (Jeffrey & Vesk, 1997). HPLC analysis also allows us to characterize the physiological condition of phytoplankton, while counts can determine whether organisms are dead or alive (Millie *et al.*, 1993). Furthermore, the composition of phytoplankton communities can be determined using HPLC derived pigment data by the means of pigment ratios (Higgins *et al.*, 2011). One of the most up to date techniques used to do this is the statistical software CHEMTAX.

CHEMTAX software uses pigments/chlorophyll-*a* ratios to characterize algal classes (Mackey *et al.*, 1996). This software has been widely used in different regions of the world oceans to characterize phytoplankton community structure (Schlüter *et al.*, 2000; Havskum *et al.*, 2004; Eker-Develi *et al.*, 2008; Kozlowski *et al.*, 2011; Araujoa *et al.*, 2017). In some studies, CHEMTAX estimates were in agreement with microscopy for major phytoplankton groups (Wright *et al.*, 1996; Llewellyn *et al.*, 2005) while not in some others (Irigoien *et al.*, 2004; Lionard *et al.*, 2008). However, the application of the CHEMTAX software to coastal and estuarine regions, is limited by the lack of known pigment ratios (Wright *et al.*, 1996; Ansotegui *et al.*, 2003; Eker-Develi *et al.*, 2012).
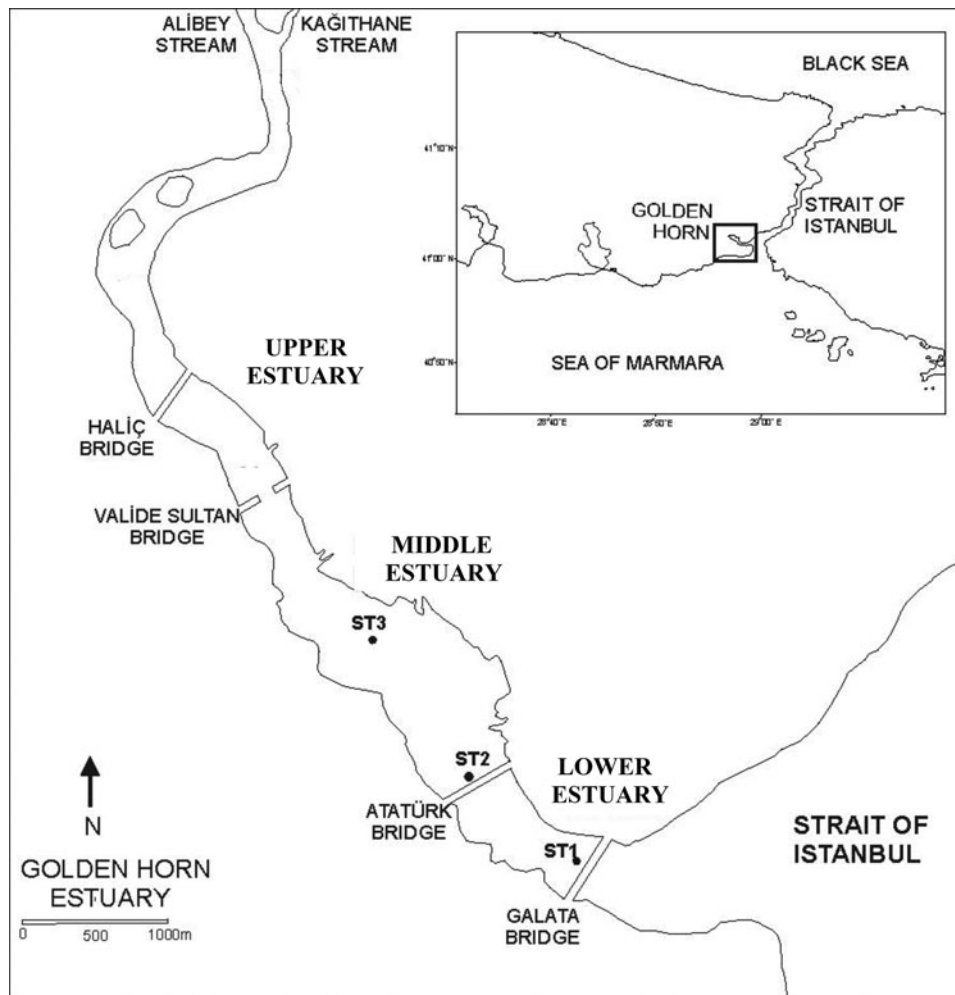
Fig. 1. Study area and sampling stations.

Estuaries are known as highly productive ecosystems, and they are transition zones between river and marine environments. Many studies of phytoplankton composition have been performed in estuaries around the Mediterranean Sea (Trigueros & Orive, 2001; Burić *et al.*, 2007; Barbosa *et al.*, 2010). Recently, studies have focused on phytoplankton communities of the Golden Horn Estuary (GHE) by microscopic analysis including the variations in phytoplankton composition (Tas *et al.*, 2009; Dursun & Tas, 2019), planktonic diatom composition (Tas, 2017; Tas & Hernández-Becerril, 2017), and algal blooms and potentially harmful species (Tas & Okus, 2011; Tas, 2015, 2019; Tas & Yilmaz, 2015; Dursun *et al.*, 2016; Tas & Lundholm, 2017). However, no study has been performed in the GHE using HPLC, despite HPLC pigment signatures being widely used in Turkish seas (Ediger *et al.*, 2006; Eker-Develi *et al.*, 2012; Agirbas *et al.*, 2017; Yücel, 2017).

The primary aim of this study was to investigate variations in phytoplankton group composition by microscopic and HPLC pigment analysis alongside associated environmental factors. A specific objective was to test the usefulness of CHEMTAX analysis for determining variations in phytoplankton group composition in the GHE for the first time.

Materials and methods

Study area and sampling strategy

The Golden Horn Estuary (GHE) is located in the north-east of the Sea of Marmara, extending in a north-west–south-east direction, ~7.5 km long and up to 700 m wide. The study area was divided into three sections based on hydrographic and bathymetric features; lower estuary (LE), middle estuary (ME) and upper estuary (UE). The maximum depth is 40 m in the LE, it decreases rapidly to 14 m in the ME and to 4 m in the UE due to high concentrations of suspended particulate material (SPM) originating from two streams, the Alibey and Kağıthane. Three stations were chosen along the study area; ST1 interacts strongly with the Strait of Istanbul (Bosphorus) and represents the LE, and ST2 and ST3 represent the ME, with an intermediate marine influence, where a bridge (Atatürk Bridge), operating on buoys, limits the upper layer circulation (Figure 1). The LE is characterized by two-layered stratification: with less saline (~18) Black Sea water above and highly saline (~38) Mediterranean water below (Ünlülata *et al.*, 1990). The upper layer extends to depths of about 25 m and the lower layer lies below ~25 m (Sur *et al.*, 2002).

The sampling period lasted for one year, from October 2018 to September 2019. Surface water samples were taken at monthly (between October and March, from June to September) and biweekly (April and May) periods from the three stations, representing the LE and ME (Figure 1). Temperature, salinity, dissolved oxygen (DO) and pH of surface water were measured using a multi-parameter probe (YSI Professional Pro Plus) from the sea surface, and water transparency was measured using a Secchi disc with 30 cm diameter. No environmental data could be measured in January due to failure of the multi-parameter probe. Seawater samples were taken from the surface (0.5 m) using 5 l Niskin bottles. For HPLC pigment analysis, surface water samples
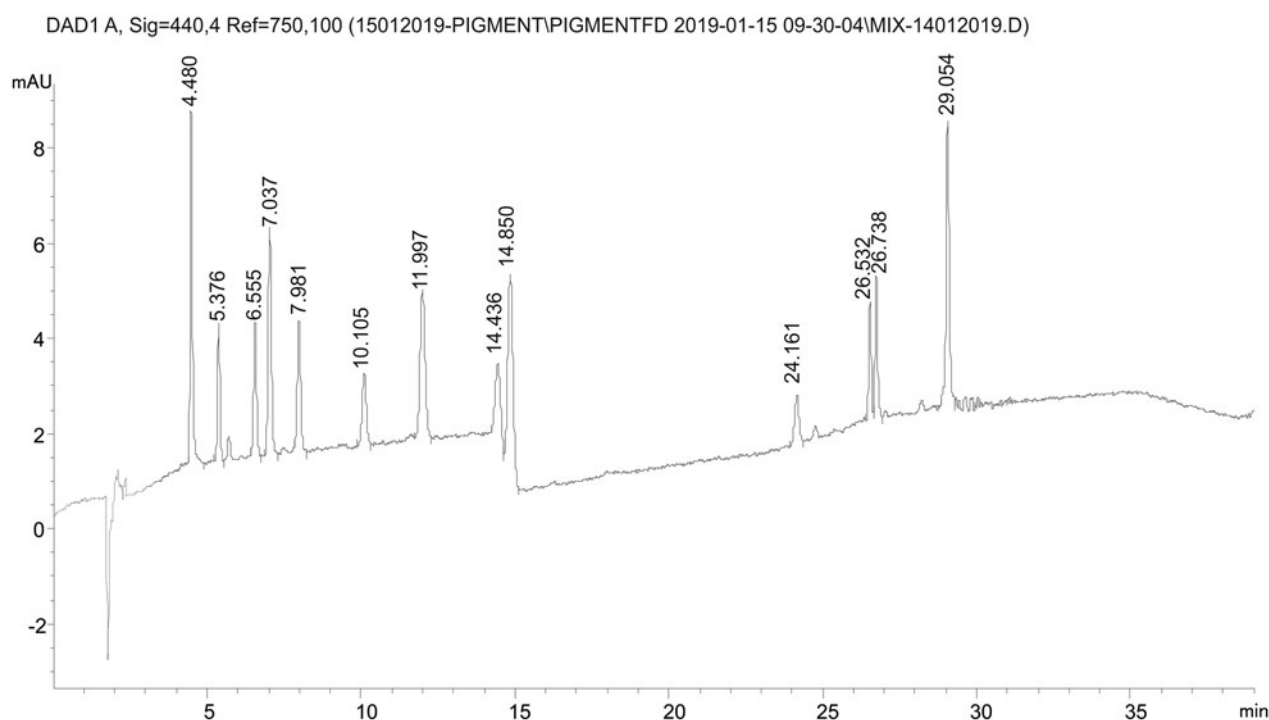
Fig. 2. HPLC chromatogram of the mixed-pigment standard.

(80–700 ml) were taken and filtered immediately onto Whatmann GF/F filters (25 mm diameter) under low vacuum (<0.7 atm) and kept frozen until extraction.

Phytoplankton analysis

For identification and enumeration of phytoplankton species, surface water samples were taken into 250 ml bottles and fixed with acidic Lugol's solution (2%) (Throndsen, 1978). Sub-samples (10–50 ml) were allowed to settle in sedimentation chambers for 24–48 h (Utermöhl, 1958). Phytoplankton cells were counted using a Leica DM IL LED inverted microscope equipped with phase contrast optics. Samples were examined at appropriate magnifications (100× to 400×) and placed into taxonomic categories such as diatoms, dinoflagellates and other phytoflagellates. Cell enumeration was generally performed on two or more transects, counting at least 300 cells in each sample and group abundances were calculated as cells per litre.

HPLC pigment analysis

The method chosen for this study (Barlow *et al.*, 1993) is a modification of the method given by Mantoura & Llewellyn (1983). According to this procedure, the frozen filters were extracted in 5 mL of 90% acetone, ultrasonicated for 1 min at 60 Hz and centrifuged at 3500 rpm for 10 min to remove cellular debris. A 500 µl aliquot of sample was filtered through a Millex-GS 0.22 µm filter into a vial and 500 µl of 1 M ammonium acetate was added; and 100 µl was injected into the HPLC Agilent 1100 series system (Agilent Technologies, Hewlett-Packard, Waldbronn, DE).

The HPLC system was calibrated for each of the pigment standards (chlorophyll-*a*, chlorophyll-*b*, chlorophyll-$c_1 + c_2$, peridinin, alloxanthin, 19′-butanoyloxyfucoxanthin, 19′-hexanoyloxyfucoxanthin, zeaxanthin, divinyl chlorophyll-*a*, fucoxanthin, diadinoxanthin, lutein and ß-carotene: DHI LAB, Denmark) and peaks were identified based on their retention times (Figure 2, Table 1). Chromatographic analyses were carried out using a Hewlett-Packard (HP) 1100 equipped with an inline degasser, quarternary

Table 1. Pigments detected in the samples listed in the order of elution in the HPLC system

Peak no.	Pigment name	Abbreviation	Elution time (min)
1	chlorophyll-$c_1 + c_2$	Chl *c*	4.48
2	peridinin	Peri	5.37
3	19′-butanoyloxyfucoxanthin	19-but	6.55
4	fucoxanthin	Fuco	7.03
5	19′-hexanoyloxyfucoxanthin	19-hex	7.98
6	diadinoxanthin	Diadino	10.10
7	alloxanthin	Allo	11.99
8	divinyl chlorophyll-*a*	Div-chl *a*	26.53
9	chlorophyll-*a*	Chl *a*	26.73
10	ß-carotene	Beta	29.05

pump, autosampler and diode-array detector; data collection and processing of chromatograms were done using the Chemstation software. Pigments were separated on a Thermo Scientific Hypersil MOS-2 C8 (150 mm × 4.6 mm, 3 µm) column. Detection wavelength was set at 440 nm with a 10 nm bandwith; the reference wavelength was 750 nm with a 100 nm bandwith. The flow rate was set at 1.0 ml min^{-1}. The mobile phases were A: 70% methanol plus 30% 1 M ammonium acetate and B:100% methanol. Gradient elution was designed at 25% B, lasted for 1 min and increased to 50% over 1 min, which was applied for 19 min. Elution was then resumed by increase to 100% B over 5 min before programming back to first conditions over 7 min. First conditions were applied for a further 7 min, resulting in a total analysis time of 39 min.

CHEMTAX analysis

On the basis of the measured pigment concentrations, the phytoplankton community composition was estimated using the

CHEMTAX software, as described by Mackey et al. (1996). CHEMTAX is a matrix-factorization software that uses factor analysis and a steepest descent algorithm to determine the best fit to the data with a given initial ratio matrix of pigment ratios (Mackey et al., 1996). Using an iterative process for a given initial ratio matrix, the software optimizes the pigment ratios for each group and applies the final ratio to the total chlorophyll-a in each sample to determine the proportion of chlorophyll-a concentration attributed to each phytoplankton group in the community. An important step to correctly estimate the contribution of different algal classes to total chlorophyll-a by CHEMTAX is the selection of the correct accessory pigment : chlorophyll-a ratios (Henriksen et al., 2002; Rodriguez et al., 2002). Therefore, pigment ratios to be used in CHEMTAX should come from the major phytoplankton species native to the area from which the samples were obtained (Mackey et al., 1996; Lewitus et al., 2005).

To determine the most appropriate input ratios for our measured concentration of marker pigments data set, 60 further pigment ratio tables were generated by multiplying each cell of initial input ratio by a randomly determined factor F. Each of the 60 ratio matrices was used and then the best 10% of results were chosen to calculate the average of the abundance estimates (Wright & Jeffrey, 2006). Besides the partial chlorophyll-a attributed to each phytoplankton group, an additional output is a new matrix of pigment : chlorophyll-a ratios resulting from the best fit. For each sample, 10 successive CHEMTAX runs were performed using the output pigment : chlorophyll-a ratio matrix of each run as input for the consequent run in order to have those ratios stabilize toward their most probable values (Latasa, 2007) (Supplementary Table S1). The three different input ratio matrices of pigment : chlorophyll-a were tested and matrices were based on pigment ratios published in the literature for oceanic (Mackey et al., 1996) and estuarine species (Schlüter et al., 2000; Lewitus et al., 2005). The results are output in terms of absolute amounts ($\mu g\, l^{-1}$) of chlorophyll-a attributed to each phytoplankton group (Supplementary Figure S1), and as a relative amount (percentage) of chlorophyll-a (Figure 8) in a sample.

Data analysis

The relationships between environmental factors, pigment types and concentrations and phytoplankton abundances were analysed by Pearson's product-moment correlation coefficients, following transformations to natural logarithms using Statistica 8.0 software. The relationships between phytoplankton cell counts obtained by microscopy and respective pigments were examined by regression analysis.

Results

Hydrography

During the study period (16 October 2018–11 September 2019), sea surface temperature (SST) showed seasonal fluctuations, varying between 7.2°C (February) and 24.7°C (July) (Figure 3). From November to May, values were consistently below 15°C. Salinity during the sampling period ranged from 8.7 (May, ST3) to 17.4 psu (April, ST1). Salinity values were generally higher at ST1 between October and May, and slightly decreased at ST2 and ST3 (Figure 3). Secchi disc depths decreased significantly from ST1 to ST3 and the highest value was measured as 7.5 m at ST1 (November), with a minimum of 1.1 m at ST3 (January) (Figure 3). DO values showed frequent variations between 5.25 (October, ST3) and 11.81 $mg\, l^{-1}$ (May, ST2), and were generally high at ST1. The pH values varied between 7.97 (March, ST3)
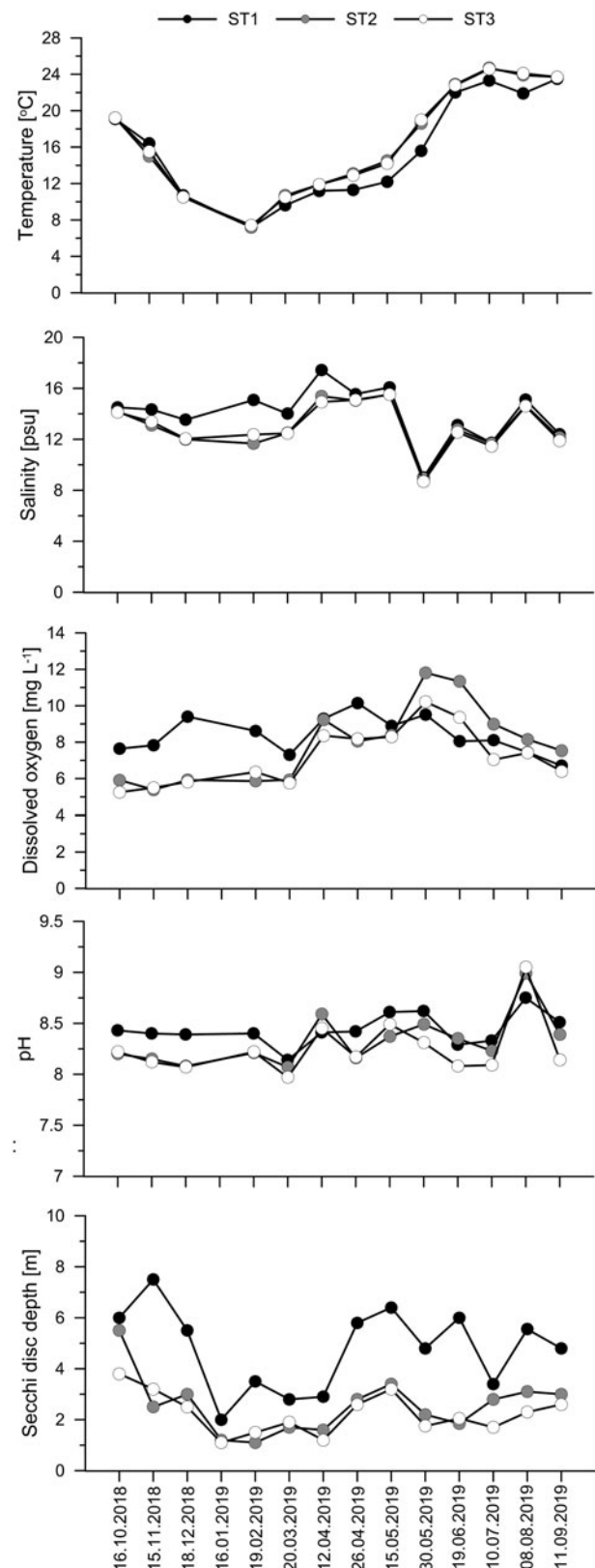

Fig. 3. Changes in some environmental factors during the study period.

and 9.05 (August, ST3) and showed no pattern over the sampling period (Figure 3).

Phytoplankton composition

A total of 80 eukaryotic phytoplankton taxa belonging to eight algal classes were identified in surface water samples collected

during the study period (Table 2). Forty-three taxa (54%) were diatoms, 29 taxa (36%) were dinoflagellates and eight taxa (10%) were other phytoflagellates, including silicoflagellates, raphidophytes, cryptomonads, chrysophytes, prasinophytes and euglenophytes. The number of diatoms and dinoflagellates, as the major groups, accounted for 90% of the total number of phytoplankton. The most diverse genera were *Chaetoceros* and *Rhizosolenia* within diatoms, and *Protoperidinium*, *Prorocentrum* and *Tripos* within dinoflagellates. The most frequent species observed during the study period were *Pseudo-nitzschia* spp., *Skeletonema* spp. and *Chaetoceros curvisetus* from diatoms; *Prorocentrum micans*, *Tripos furca*, *T. fusus* from dinoflagellates; *Plagioselmis prolonga* from cryptomonads and *Heterosigma akashiwo* from raphidophytes (Table 2).

Total phytoplankton abundance showed seasonal and spatial fluctuations and was relatively low (49×10^3–350×10^3 cells l^{-1}) between October and March, while it was high (11×10^3–$30,000 \times 10^3$ cells l^{-1}) between April and July (Figure 4). The highest cell abundance ($\sim 27,500 \times 10^3$ cells l^{-1}) was detected at ST2 in June (Figure 4). 87% of the cell abundances were lower than 10^4 cells l^{-1}, while 7% were between 10^4 and 10^5 cells l^{-1}, and 4% were between 10^5 and 10^6 cells l^{-1}. Only 2% of cell abundances were higher than 10^6 cells l^{-1} (Table 2).

Group composition based on cell abundance varied between the sampling months of the study period. Diatoms were clearly abundant between April and May, while cryptomonads and raphidophytes were more abundant from June to September at ST2 and ST3 (Figure 5). The average contribution of diatom abundance to total phytoplankton decreased from ST1 to ST3 (41 to 25%), while the average contribution of dinoflagellate and other phytoflagellate abundances increased (59 to 75%) (Figure 6).

Diatoms

The majority of phytoplankton taxa (43 taxa) were diatoms. The most diverse genera were *Chaetoceros* and *Rhizosolenia*; and the most abundant species were *Pseudo-nitzschia* spp., *Skeletonema* spp. and *Chaetoceros curvisetus*. In general, diatom abundance displayed marked seasonal differences and their highest abundance was observed between April and May in the study area (Figure 5). The maximum diatom abundance ($\sim 11,000 \times 10^3$ cells l^{-1}) was found in May, dominated by *Skeletonema* spp. at ST3 ($\sim 10,750 \times 10^3$ cells l^{-1}) (Figure 5). *Skeletonema* spp. reached $\sim 8100 \times 10^3$ cells l^{-1} at ST2 in May, as well (Figure 5). Other common diatoms were *Pseudo-nitzschia* spp. and *Chaetoceros curvisetus* in the study region with a highest abundance of 520×10^3 cells l^{-1} at ST1 in May, and 325×10^3 cells l^{-1} at ST3 in April, respectively. Diatom abundance was negatively correlated with salinity ($P < 0.05$) and there was a strong positive correlation between diatom abundance and DO ($P < 0.01$) (Table 3). The mean annual contribution of diatoms to total phytoplankton abundance was 31.5% (Figure 6).

Dinoflagellates

Dinoflagellates were the second major group (29 taxa) of the phytoplankton community. *Protoperidinium*, *Prorocentrum* and *Tripos* were the most diverse genera. Dinoflagellate abundance was generally lower, compared with the other groups. Their highest abundances were found at ST2 and ST3 (Figure 5). The highest dinoflagellate abundance (214×10^3 cells l^{-1}) was observed in June, dominated by *Scrippsiella acuminata* at ST2 (142×10^3 cells l^{-1}) (Figure 5). The same species reached 34×10^3 cells l^{-1} at ST3 in June, as well. Other dinoflagellate species, *Prorocentrum scutellum* and *Heterocapsa triquetra* reached 17×10^3 cells l^{-1} in December and 16×10^3 cells l^{-1} in June, respectively (Figure 5).

Dinoflagellate abundance was weakly positively correlated with DO ($P < 0.05$), while no correlation was found between salinity, temperature and dinoflagellate abundance in the study period (Table 3). The mean annual contribution of dinoflagellates to total phytoplankton abundance was 6.5% (Figure 6).

Other phytoflagellates

A total of eight phytoflagellate taxa belonging to six algal classes were observed in surface water collected during this work. *Plagioselmis prolonga* (Cryptophyceae), *Heterosigma akashiwo* (Raphidophyceae), *Apedinella* sp. (Chrysophyceae) and *Eutreptiella* sp. (Euglenophyceae) were the most common species in the study area. *Plagioselmis prolonga*, a bloom-forming cryptomonad, was frequently observed and its highest abundance reached 540×10^3 cells l^{-1} at ST3 in August (Figure 5). Cryptomonad abundance was positively correlated with salinity ($P < 0.05$) and pH ($P < 0.01$) during the study period (Table 3). The mean annual contribution of cryptomonads to total phytoplankton abundance was 34.6% (Figure 6). Another bloom-forming species was *Heterosigma akashiwo*, and it was commonly observed from June to September. A bloom of *H. akashiwo* occurred at ST2 in June with maximum abundance of $27,000 \times 10^3$ cells l^{-1} (Figure 5). Raphidophyte abundance was positively correlated with temperature ($P < 0.05$, Table 3). The mean annual contribution of raphidophytes to total phytoplankton abundance was 20.5% (Figure 6). Euglenophytes were generally observed between March and September (Figure 5). The highest abundance of *Eutreptiella* sp. was found as 432×10^3 cells l^{-1} at ST2 and ST3 in April. Euglenophyte abundance was negatively correlated with Secchi depth ($P < 0.05$) and positively correlated with DO ($P < 0.05$) during the study period (Table 3). *Apedinella* sp. appeared only in April and reached 1100×10^3 cells l^{-1} at station ST1 and ST2 (Figure 5). Chrysophyte abundance was positively correlated with salinity ($P < 0.05$, Table 3). The mean annual contributions of chrysophytes, euglenophytes, silicoflagellates and prasinophytes to the total phytoplankton abundance were 4.5, 1.8, 0.6 and 0.1%, respectively (Figure 6).

Distribution of marker pigments

Chlorophyll-*a* and nine other marker pigments were identified in the Golden Horn Estuary (Table 1). Lutein, zeaxanthin and chlorophyll-*b* were not detected at any time and station. Chlorophyll-*a* and marker pigment (e.g. fucoxanthin and peridinin) concentrations for all stations and all sampling dates are presented in Figures 4 and 7.

Chlorophyll-*a* concentrations ranged between 0.12 and 19.49 $\mu g \, l^{-1}$ in surface waters during the study period (Figure 4). The highest chlorophyll-*a* concentrations (19.49 and 14.24 $\mu g \, l^{-1}$) were observed at ST3 and ST2 during July. Chlorophyll-*a* values were generally lower ($< 1.5 \, \mu g \, l^{-1}$) from October to June, and increased markedly between July and September (Figure 4).

In addition to chlorophyll-*a*, concentrations of two other marker pigments, fucoxanthin and peridinin, being the major markers of diatoms and dinoflagellates, respectively, were identified at the study region. The concentration of fucoxanthin, which was notably high ($> 0.15 \, \mu g \, l^{-1}$) from April to September, was observed to be low ($< 0.05 \, \mu g \, l^{-1}$) between October and March (Figure 7). Its concentration in surface water varied between 0.05 and 3.41 $\mu g \, l^{-1}$. Fucoxanthin concentrations were generally low ($< 0.98 \, \mu g \, l^{-1}$) at ST1, and the maximum fucoxanthin values were measured at ST2 (3.41 $\mu g \, L^{-1}$) in June and at ST3 (2.47 $\mu g \, l^{-1}$) in July, respectively (Figure 7).

Peridinin concentrations were low from October to May (0.06–0.30 $\mu g \, l^{-1}$), and values were consistently below 0.30 $\mu g \, l^{-1}$

Table 2. List of phytoplankton taxa identified during the study period and the groups of abundance based on the mean cell number

Taxa	Sampling periods													
	Oct.	Nov.	Dec.	Jan.	Feb.	Mar.	Apr-I	Apr-II	May-I	May-II	June	July	Aug.	Sep.
Bacillariophyceae														
Actinocyclus sp.	–	–	–	–	A	–	–	–	–	–	–	–	–	–
Aulacoseira granulata	–	–	–	A	–	–	–	–	–	–	–	–	–	–
Asterionellopsis glacialis	–	–	A	–	–	–	–	–	–	–	–	–	–	–
Cerataulina pelagica	A	–	–	–	–	–	–	–	–	–	–	–	–	–
Chaetoceros aequatorialis	A	–	–	–	–	–	–	–	–	–	–	–	–	–
Chaetoceros affinis	–	–	–	A	–	–	–	–	–	–	B	–	–	–
Chaetoceros curvisetus	–	B	–	A	–	A	B	D	C	–	–	–	–	–
Chaetoceros decipiens	–	A	–	–	–	–	–	–	B	–	–	–	–	–
Chaetoceros diadema	A	–	–	–	–	–	–	–	–	–	–	–	–	–
Chaetoceros didymus	–	–	–	–	–	–	–	–	–	–	–	–	A	–
Chaetoceros lorenzianus	A	–	–	–	–	–	–	–	–	–	–	–	–	–
Chaetoceros teres	–	–	–	–	–	–	–	–	–	–	–	–	B	–
Chaetoceros tortissimus	A	–	–	–	–	–	–	–	–	–	–	–	–	–
Chaetoceros socialis	–	–	–	–	–	–	–	–	–	–	–	–	–	–
Chaetoceros sp.	B	A	A	B	A	–	A	–	–	–	–	A	B	–
Coscinodiscus sp.	A	A	A	A	–	–	A	–	–	–	–	–	–	–
Cylindrotheca closterium	C	A	–	–	–	–	–	–	–	–	A	–	B	B
Dactyliosolen fragilissimus	–	–	–	–	A	–	–	–	–	–	B	–	–	–
Ditylum brightwellii	–	–	A	A	–	–	–	–	–	–	–	–	–	–
Guinardia delicatula	A	–	A	B	–	–	A	–	–	–	B	–	–	–
Guinardia striata	–	–	–	–	–	–	–	–	–	–	–	A	–	–
Hemialus hauckii	A	–	–	–	–	–	–	–	–	–	–	–	–	–
Lauderia annulata	A	–	–	–	–	–	–	–	–	–	–	–	–	–
Leptocylindrus danicus	–	–	B	B	A	–	–	–	–	–	B	–	A	B
Leptocylindrus minimus	A	–	–	B	–	–	–	–	–	–	–	–	–	–
Licmophora sp.	–	–	–	–	–	–	–	–	–	–	–	–	–	A
Melosira moniligera	A	–	–	–	–	–	–	–	–	–	–	–	–	–
Meuniera membranacea	–	–	–	A	–	–	–	–	–	–	–	–	–	–
Navicula sp.	A	–	–	–	–	–	–	–	–	–	–	–	–	–
Nitzschia longissima	A	A	A	A	–	A	A	A	–	–	–	–	–	–

Nitzschia sp.	–	–	A	–	–	–	–	–	–	–	–	–	–	–
Pleurosigma normanii	–	A	A	–	–	–	–	–	–	–	–	–	–	–
Pleurosigma sp.	–	A	–	–	–	–	–	–	–	–	–	–	–	–
Proboscia alata	B	–	A	A	–	–	A	–	–	–	–	–	A	A
Pseudo-nitzschia spp.	B	A	–	A	–	A	C	D	D	C	C	A	B	A
Pseudosolenia calcar-avis	A	A	–	A	–	–	–	–	–	–	–	–	–	–
Rhizosolenia hebetata	A	A	A	–	–	–	–	–	–	–	–	A	B	A
Rhizosolenia setigera	–	–	–	–	–	–	A	–	–	–	B	–	–	–
Skeletonema sp.	A	–	A	B	–	–	B	D	E	E	C	–	B	B
Stellarima stellaris	–	–	–	A	–	–	–	–	–	–	–	–	–	–
Striatella unipunctata	–	–	–	–	–	–	A	–	–	–	–	–	–	–
Thalassionema nitzschioides	–	A	A	A	–	A	A	–	–	–	B	–	–	A
Thalassiosira rotula	–	–	B	A	–	–	A	A	–	–	–	–	–	–
Dinophyceae														
Dinophysis acuminata	–	–	–	–	–	–	–	A	–	–	–	–	–	–
Dinophysis acuta	–	–	–	–	–	–	–	–	–	–	–	A	–	A
Dinophysis caudata	–	A	–	–	–	–	–	–	–	–	–	–	–	–
Diplopsalis lenticula	A	–	–	–	–	–	–	–	–	–	–	–	–	–
Gyrodinium sp.	A	A	A	–	A	A	A	A	A	–	A	A	–	–
Heterocapsa triquetra	–	–	–	–	–	A	–	A	C	–	C	–	–	–
Katodinium glaucum	–	–	–	–	–	–	–	–	–	–	–	–	–	A
Noctiluca scintillans	–	–	–	–	–	A	–	–	A	A	–	–	–	–
Oxytoxum scolapax	–	–	–	–	–	–	A	–	–	–	–	–	–	–
Phalacroma rotundatum	–	A	–	A	–	–	–	–	–	–	A	A	–	–
Polykrikos schwartzii	–	–	A	–	A	–	–	–	–	–	–	–	–	–
Prorocentrum cordatum	A	–	–	–	–	–	–	–	–	–	B	A	B	A
Prorocentrum compressum	–	A	A	–	–	–	–	–	–	A	A	–	–	A
Prorocentrum micans	A	A	B	B	A	A	B	A	–	A	B	A	A	B
Prorocentrum scutellum	–	A	B	B	–	–	A	–	–	–	–	–	–	–
Protoperidinium bipes	–	–	–	–	–	–	–	A	–	–	–	–	–	–
Protoperidinium brevipes	–	–	–	–	–	–	–	A	–	–	–	–	–	–
Protoperidinium conicum	–	–	–	–	–	–	A	–	–	–	–	–	–	–
Protoperidinium depressum	A	–	–	A	A	–	–	–	–	A	–	–	–	–
Protoperidinium divergens	–	–	–	–	–	–	–	–	–	–	–	A	–	–

Table 2. (*Continued.*)

Taxa	Oct.	Nov.	Dec.	Jan.	Feb.	Mar.	Apr-I	Apr-II	May-I	May-II	June	July	Aug.	Sep.
										Sampling periods				
Protoperidinium pellucidum	–	–	–	–	–	–	–	–	–	–	–	–	–	A
Protoperidinium steinii	A	A	A	A	–	–	A	–	–	–	A	–	–	–
Protoperidinium sp.	A	A	A	A	A	–	–	–	–	–	–	A	–	–
Scrippsiella acuminata	–	–	–	–	–	–	–	–	A	B	C	–	–	A
Tripos furca	–	A	A	A	–	–	A	–	–	A	B	A	–	A
Tripos fusus	A	A	A	A	–	A	A	–	–	A	B	A	–	A
Tripos horridus	–	–	–	A	–	–	–	–	–	–	–	–	–	–
Tripos lineatus	–	–	–	–	–	–	A	–	–	–	–	–	–	–
Tripos muelleri	–	A	–	–	–	–	A	A	–	–	A	–	–	–
Dictyochophyceae														
Dictyocha fibula	–	–	–	A	–	–	–	–	–	–	–	–	–	–
Dictyocha speculum	–	A	A	A	A	–	A	–	–	–	–	–	–	–
Octactis octonaria	–	A	A	A	–	–	–	–	–	–	–	–	–	–
Raphidophyceae														
Heterosigma akashiwo	–	–	–	–	–	–	–	–	–	–	E	D	E	E
Cryptophyceae														
Plagioselmis prolonga	C	C	C	C	C	C	D	C	C	–	–	D	D	D
Chrysophyceae														
Apedinella sp.	–	–	–	–	–	–	E	C	–	–	–	–	–	–
Prasinophyceae														
Pyramimonas grossii	B	–	–	–	–	–	–	–	–	–	–	–	–	–
Euglenophyceae														
Eutreptiella sp.	–	–	–	–	–	A	D	–	B	D	C	A	B	B

The groups of abundance (cells l^{-1}) refers to the following: A = <10^3; B = 10^3–10^4; C = 10^4–10^5; D = 10^5–10^6; E = >10^6; (–), absent.
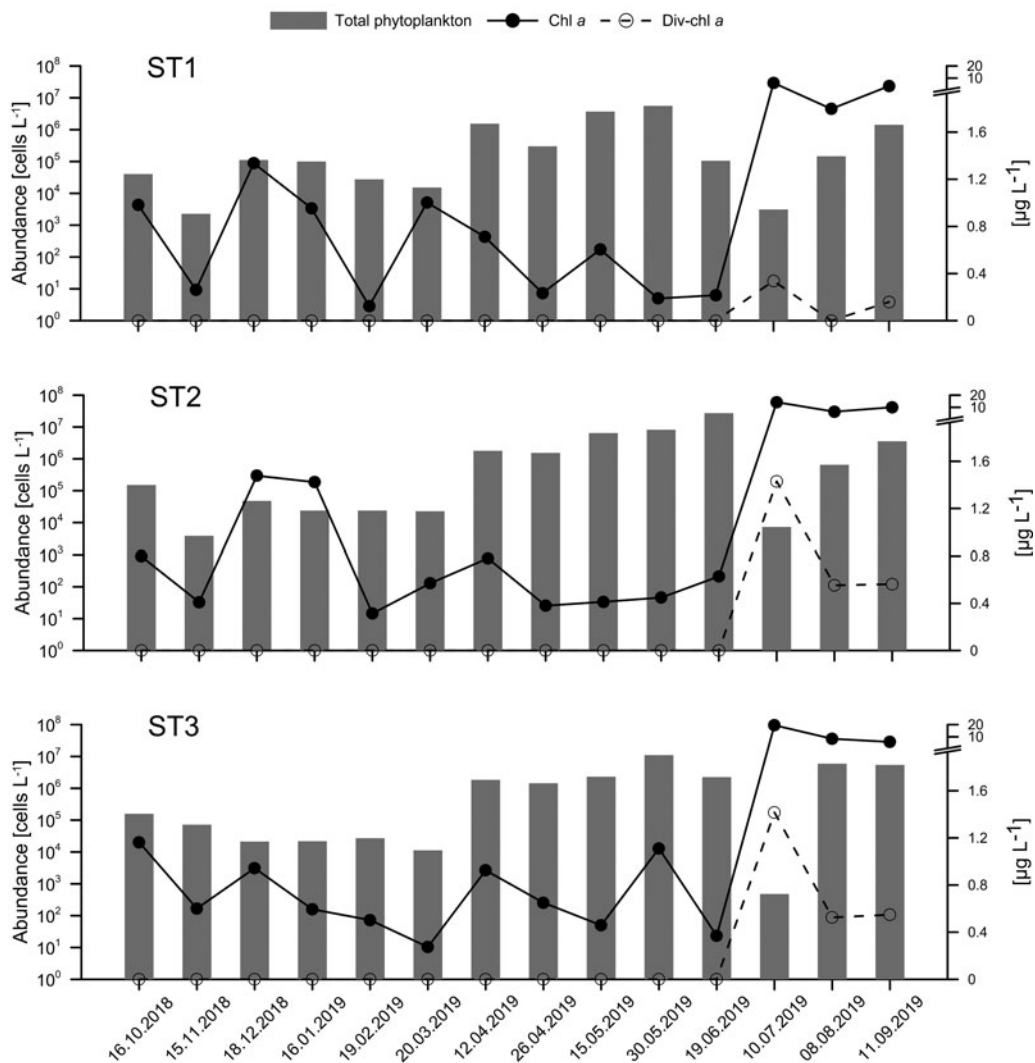
Fig. 4. Distribution of total phytoplankton abundance, chlorophyll-*a* and divinyl chlorophyll-*a* in the GHE during the study period.

(Figure 7). Its concentration in the surface water changed from 0.06 to 4.66 µg l^{-1} during the study period. Peridinin concentrations were generally low at ST1 (<0.4 µg l^{-1}), with the highest concentration being measured at ST2 (4.66 µg l^{-1}) in June (Figure 7).

Alloxanthin was mostly observed between April and July, and its concentration varied between 0.05 and 0.47 µg l^{-1} (Figure 7). The maximum alloxanthin value was detected at ST2 in June. Chlorophyll-$c_1 + c_2$ was generally observed during the study period and concentrations varied between 0.03 and 0.76 µg l^{-1}. The maximum chlorophyll-$c_1 + c_2$ value was measured at ST2 in June (Figure 7). Diadinoxanthin concentrations changed between 0.09 and 0.36 µg l^{-1} (Figure 7) and the maximum value was measured at ST2 in June. ß-carotene was mostly detected from October to January, and from July to September, and its concentration ranged between 0.05 and 0.31 µg l^{-1} (Figure 7). The maximum ß-carotene values were observed at ST2 (0.31 and 0.30 µg l^{-1}) in December and January, respectively. Other accessory pigments, i.e. divinyl chlorophyll-*a* (0.34–1.43 µg l^{-1}), 19′-butanoyloxyfucoxanthin (0.35–10.75 µg l^{-1}) and 19′-hexanoyloxyfucoxanthin (0.07–0.66 µg l^{-1}), an indicator of prochlorophytes, chrysophytes and prymnesiophytes, were detected but they were not consistently present.

CHEMTAX derived estimations

The CHEMTAX analysis indicated that dinoflagellates were the dominant planktonic algae calculated based on Matrix 1 and

Matrix 2 (Figure 8A, B). Dinoflagellates were the most dominant species at all stations except from April to July, representing 60–99% of the phytoplankton composition and contributing on average 62% of total chlorophyll-*a* in Matrix 1 (Figure 8A). Cryptomonads were identified as the second dominant algal group, contributing on average 35% to total chlorophyll-*a* and diatoms contributed on average 3% to total phytoplankton composition. The average contribution of dinoflagellate and cryptomonad abundances to total phytoplankton showed minor variations from ST1 to ST3.

The calculation based on Matrix 2 showed that dinoflagellates were the dominant taxa at all stations except from April to July, accounting for 61–100% of the phytoplankton composition and contributing on average 62% of total chlorophyll-*a* (Figure 8B). Diatoms and cryptomonads contributed on average 30.3 and 7.7% to total chlorophyll-*a*, respectively. The average contribution of dinoflagellate abundance to total phytoplankton inreased from ST1 to ST3 (59 to 67%), while the average contribution of diatom abundance decreased (34 to 25%).

The results based on the above two matrices (Matrix 1 and Matrix 2) substantially overestimated dinoflagellates but considerably underestimated diatoms (Figure 8A, B). During the estimation process, it was determined that as the shared pigments of diatoms and dinoflagellates, the increase or decrease in diadinoxanthin and chlorophyll-$c_1 + c_2$ to chlorophyll-*a* ratio could affect the estimation of diatom composition, leading to the underestimation of diatoms and overestimation of dinoflagellates.
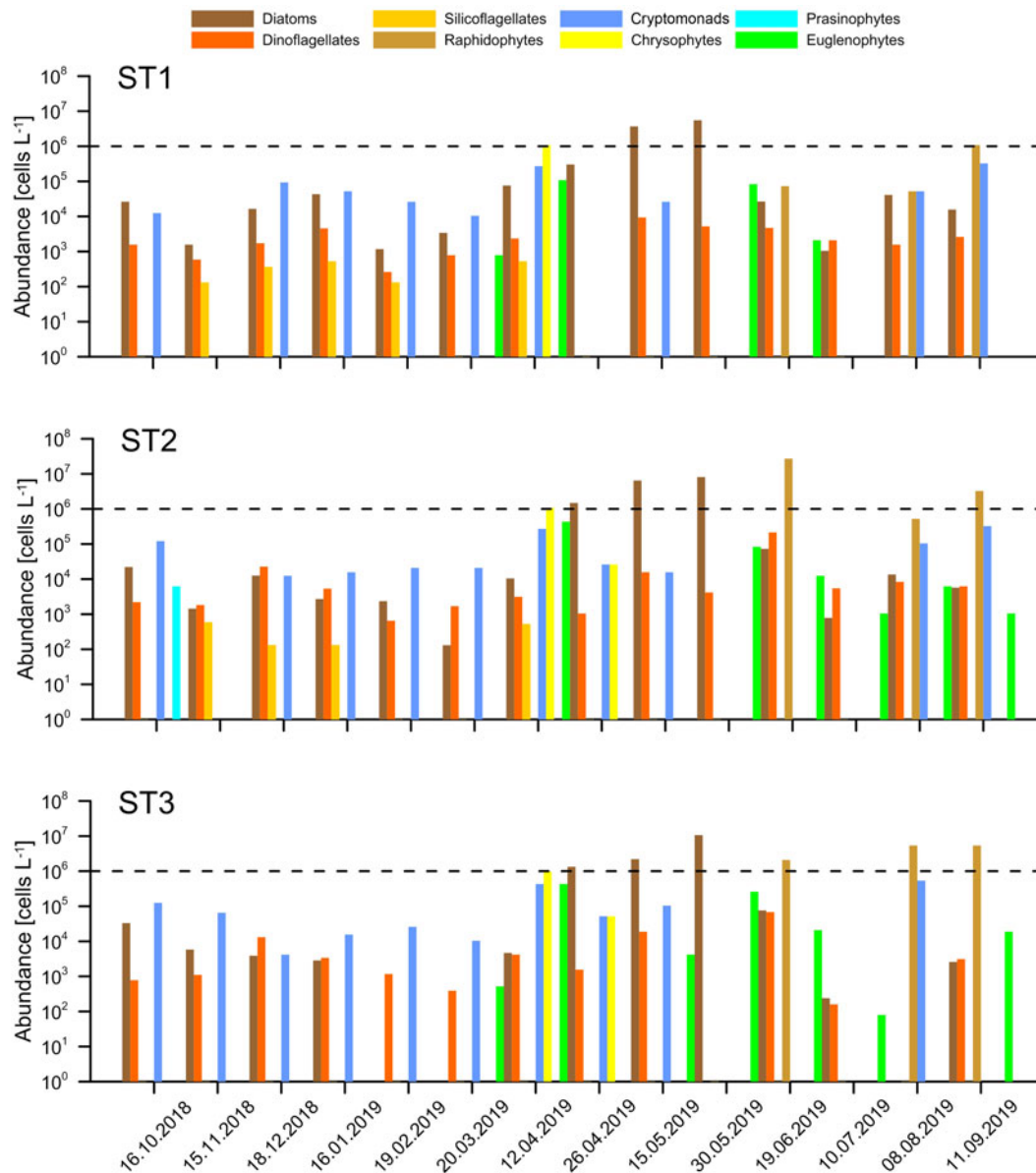
Fig. 5. Spatio-temporal variations in abundance of phytoplankton groups during the study period (dashed lines show the lowest limit of bloom density).

Based on the above results, we reduced the ratio of fucoxanthin and diadinoxanthin of diatoms in Matrix 1 and Matrix 2, and increased the ratio of chlorophyll-$c_1 + c_2$ of diatoms. Final adjustments were conducted to obtain Matrix 3, whose results were more similar than Matrix 1 and Matrix 2 to those from microscopic observations (Figure 8C). CHEMTAX analysis based on Matrix 3 identified diatoms as the dominant algal group, except in April at ST1 and ST2, and in June at ST3. Diatoms represented 68–100% of the phytoplankton composition with a contribution on average of 86% of total chlorophyll-*a* (Figure 8C). However, dinoflagellates and cryptomonads contributed on average 30.3% and 7.7% to total chlorophyll-*a*, respectively. The contribution of diatoms to the phytoplankton community showed higher values at ST1 and ST3 (88% and 87%) when compared with ST2 (83%). Dinoflagellates were more abundant at ST2 (11%), than ST1 and ST3 (8.1 and 8.5%). The relative distribution of cryptomonads increased from ST1 (3.8%) to ST3 (5%).

Discussion

The validity of using pigment signatures detected by HPLC to estimate phytoplankton group composition was tested for the Mediterranean Sea (Thyssen *et al.*, 2011; Yücel, 2017) and Black Sea (Ediger *et al.*, 2006; Eker-Develi *et al.*, 2012; Agirbas *et al.*, 2015, 2017). Although there have been many studies on phytoplankton in the Golden Horn Estuary (Tas *et al.*, 2009; Tas & Okus, 2011; Tas & Yilmaz, 2015; Dursun & Tas, 2019; Tas, 2019) based on microscopic examination, the phytoplankton group composition had not yet been evaluated by HPLC pigment analysis in this region.

In this study, the highest abundances in total phytoplankton were observed between April and September, as shown by microscopic analysis. The abundance pattern displayed seasonal variations in this study that are similar to previous studies (Tas *et al.*, 2009; Tas & Yilmaz, 2015; Dursun & Tas, 2019). Phytoplankton studies performed in estuaries show that environmental factors such as salinity, temperature, Secchi depth and adaptation to the environmental conditions play a major role in seasonal variations of phytoplankton in terms of diversity and abundance (Burić *et al.*, 2007; Barbosa *et al.*, 2010; Jasprica *et al.*, 2012). Similar relationships were demonstrated in previous studies in the GHE by Tas *et al.* (2009, 2016) and Dursun & Tas (2019), but no clear relationships were found between the environmental factors and total phytoplankton abundance measured
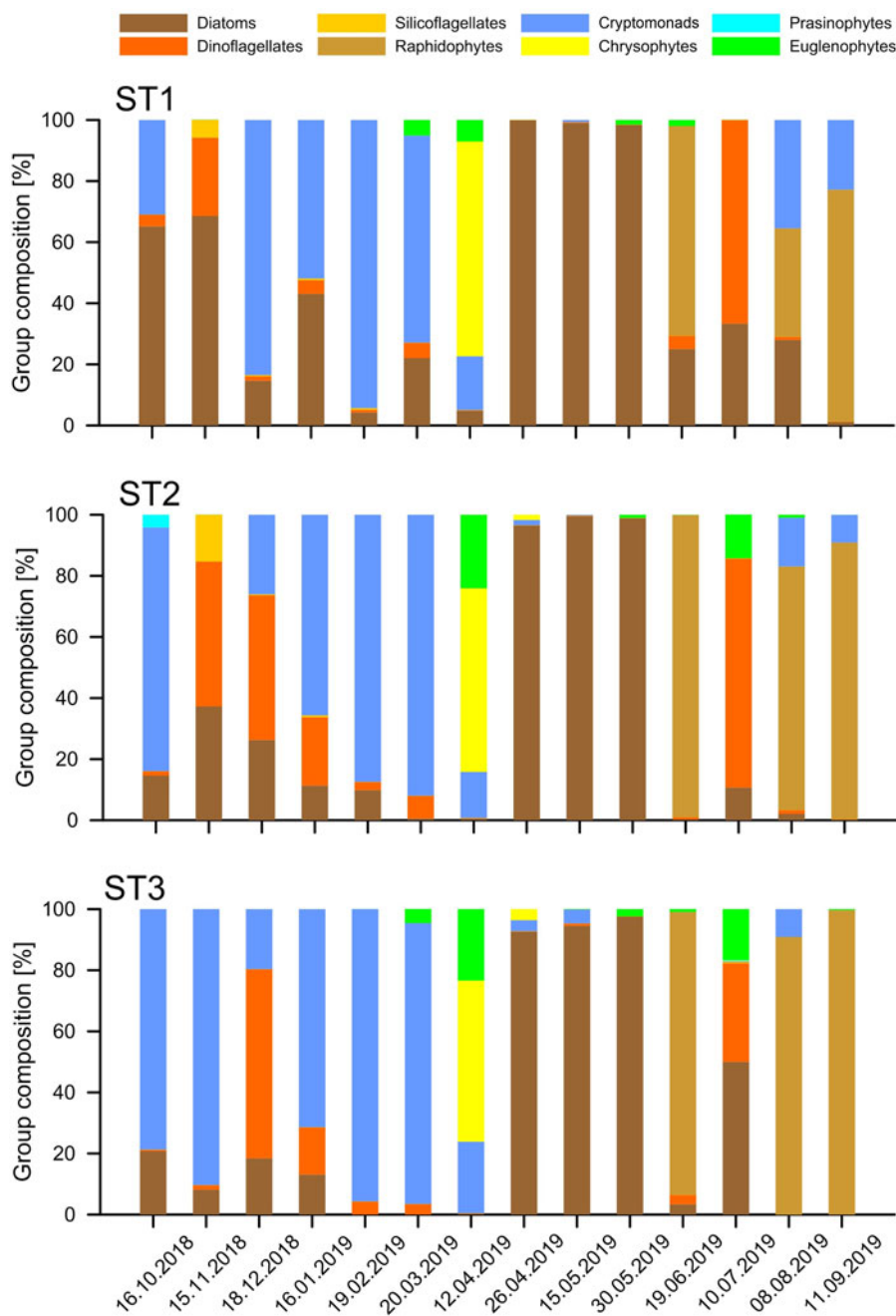
Fig. 6. Relative contribution of phytoplankton groups to the total abundance during the study period.

in this study. However, it is known that phytoplankton abundance is increased in coastal areas and estuarine ecosystems by eutrophication (Smith *et al.*, 1999). As noted in previous studies in the GHE (Tas *et al.*, 2009; Tas & Okus, 2011; Tas & Yilmaz, 2015), nutrient inputs might cause an increase in phytoplankton abundance in the GHE, particularly in summer and spring.

The number of phytoplankton taxa observed during this study was similar to that of Dursun & Tas (2019), but lower than previous studies of the GHE by Tas *et al.* (2009) and Tas & Yilmaz (2015). The contribution of diatoms and dinoflagellates to the total number of species was higher (90%), and that of other phytoflagellates was relatively lower (10%) than previous studies performed by Dursun & Tas (2019) in the GHE and by Jasprica *et al.* (2012) in the Eastern Adriatic estuary (Neretva River). This inconsistency between studies was probably due to the differences in the total number of samples, sampling periods and frequencies. Burić *et al.* (2007) stated for the Zrmanja, Adriatic Sea that diatoms dominated in spring, while dinoflagellates and other phytoflagellates dominated in summer. Our results were generally

consistent with Burić *et al.* (2007) and this indicates that phytoplankton group composition in the GHE may change rapidly depending on environmental conditions.

The highest phytoplankton abundance was found at ST2 in June, although some higher abundances were observed at all stations particularly in May. Furthermore, chlorophyll-*a* values were generally observed to be higher from July to September at all stations and the maximum chlorophyll-*a* value ($19.50 \, \mu g \, l^{-1}$) was measured at ST3 in July. In contrast to the study performed by Silva *et al.* (2008), who found a good relationship between total phytoplankton abundance and HPLC derived chlorophyll-*a* concentrations in Lisbon Bay, Portugal. The results of this study showed no relation between chlorophyll-*a* concentrations detected by HPLC and total phytoplankton abundance. The same conclusion was reported by Pérez *et al.* (2006) and this situation may be caused by the constitution of the high portion of phytoplankton by picoplanktonic species which could not be identified by microscopy. Thus, all phytoplankton groups could not be identified by microscopic analysis in the study area. Flow cytometry may provide

Table 3. Pearson Product-Moment correlations between environmental parameters, pigment types and their concentrations, and phytoplankton group abundances

	Diatoms	Dinoflagellates	Raphidophytes	Cryptomonads	Chrysophytes	Euglenophytes
Secchi depth						−0.332*
Salinity	−0.404*			0.321*	0.392*	
Temperature			0.319*			
DO	0.498**	0.375*				0.327*
pH				0.510**		
Peridinin		0.819**				
19′-but			0.896**			
Fuco			0.558**			
19′-hex					0.762**	
Alloxanthin		0.729**				

Statistically significant correlations are indicated by symbols: N = 42; *$P < 0.05$, **$P < 0.01$.
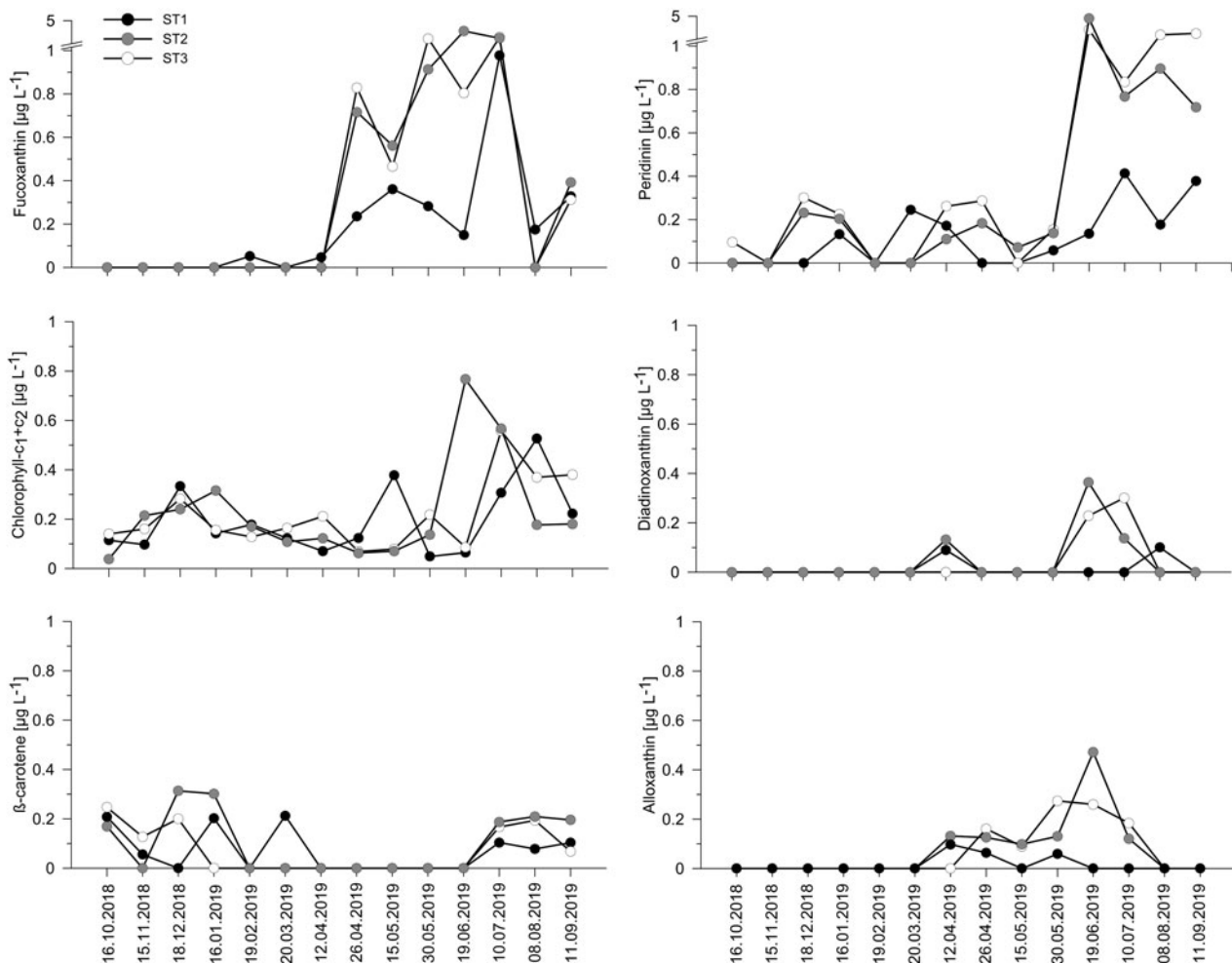
Fig. 7. Distributions of surface pigment concentrations in the Golden Horn Estuary.

additional information regarding the cell size distribution of the plankton community. In particular the picoplankton component can be studied in great detail (Olson *et al.*, 1990; Campbell & Vaulot, 1993; Veldhuis & Kraay, 2000). In addition to this, estimation of the abundance of the total phytoplankton community based on chlorophyll-*a* only can be unreliable because of the algal cells' adaptation strategy to varying light levels of changing their pigment content (Everitt *et al.*, 1990; Veldhuis & Kraay, 1990).

Higher divinyl chlorophyll-*a* values (0.34–1.43 µg l^{-1}) were measured from July to September (Figure 4) and these findings may indicate the existence of prochlorophytes, which are photosynthetic picoplankton. Gibb *et al.* (2000) stated that higher divinyl chlorophyll-*a* values were detected when the sea surface temperature (SST) values were greater than 15°C and our findings were consistent (SST >23°C, from July to September; Figure 3) with the results of that study. However, in this study, lutein,
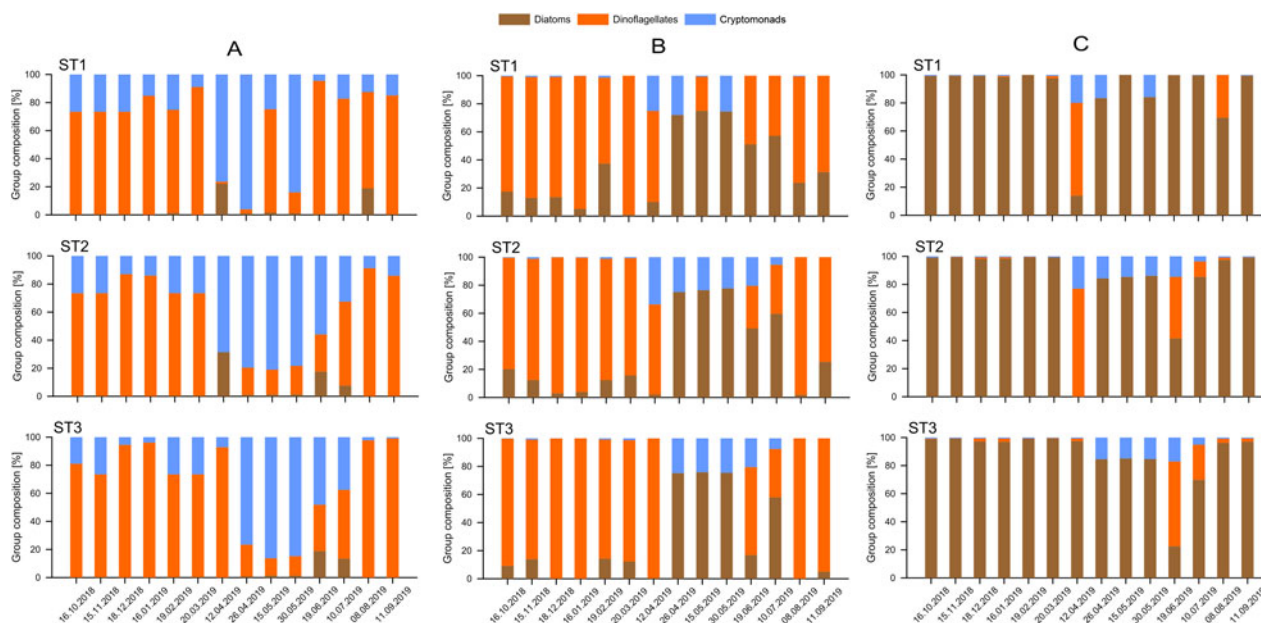
Fig. 8. The relative contribution of groups to phytoplankton composition, calculated using different pigment matrices in CHEMTAX. Matrix 1 (A), Matrix 2 (B), Matrix 3 (C).

zeaxanthin and chlorophyll-*b* pigments, which were commonly stated as the markers of the picoplanktonic species (Eker-Develi *et al.*, 2012; Agirbas *et al.*, 2015), were not detected. However, not all picoplanktonic groups (for example, *Prochlorococcus* spp.) carry lutein, zeaxanthin and chlorophyll-*b* markers. This was highlighted by Veldhuis & Kraay (2004) who showed that *Prochlorococcus* spp. has only divinyl chlorophyll-*a* pigment instead of chlorophyll-*a* and does not carry lutein and zeaxanthin.

Comparative studies generally show a good relationship between microscopy and HPLC analysis for diatom species (especially larger ones), but the correlation is lower for dinoflagellates, raphidophytes and crysophytes due to the shared marker pigments (Zapata *et al.*, 2004; Eker-Develi *et al.*, 2012; Agirbas *et al.*, 2015). Comparison of fucoxanthin *vs* diatom abundance indicates that the relationship was not found in this study. It has been reported by Agirbas *et al.* (2017) for the Black Sea and by Seoane *et al.* (2011) for the Bay of Biscay (Basque coast, northern Spain) that diatoms were the most abundant microplanktonic group in summer, with the highest diatom abundances being observed during spring (April and May) in this study, similar to Totti's (2000) observations for the middle Adriatic. Moreover, the concentration of fucoxanthin was found to be maximum in June and July in this study which differs from the data presented by Ansotegui *et al.* (2003) when the maximum fucoxanthin concentration was found in late winter in a Spanish estuary. This inconsistency might be the result of the peak of fucoxanthin possibly originating from nanoplanktonic non-diatom species in the study region (Krivokapić *et al.*, 2018). All these findings suggest that fucoxanthin as a marker pigment did not work well for the diatom community and demonstrates the need for microscopic confirmation to fully characterize peak events in the GHE.

Generally, low concentrations of peridinin were detected with the HPLC analysis, in correspondence to the low abundance of dinoflagellates detected by microscopic analysis. The highest dinoflagellate abundance $(214 \times 10^3$ cells $l^{-1})$ was observed in June, in accordance with the highest peridinin concentration $(4.66 \, \mu g \, l^{-1})$ at the same period. The maximum dinoflagellate abundance was dominated by *Scrippsiella acuminata* in the study region, which was indicated as the carrier of peridinin by several studies (Zhang *et al.*, 2000; Wong & Wong, 2009;

Islabão *et al.*, 2016). Thus, comparison of marker pigment values and microscopic cell counts indicates that a significant relationship between peridinin and dinoflagellate abundance was observed in the study region (Table 3, N = 42, $P < 0.01$, $r = 0.819$).

Cryptomonads were one of the most frequent groups in the phytoplankton community from October to April in the GHE, as reported in other estuarine and coastal waters (Brunet & Lizon, 2003; Carreto *et al.*, 2003; Garibotti *et al.*, 2003; Seoane *et al.*, 2006). However, alloxanthin, which indicates the presence of crytocryptomonads (Jeffrey & Vesk, 1997), was mostly observed between April and July. The maximum value was detected in June and no correlation was found between alloxanthin and cryptomonad abundance (Table 3). Moreover, dinoflagellate abundance was highly correlated with alloxanthin values (Table 3, N = 42, $P < 0.01$, $r = 0.729$). A possible explanation of this situation might be the presence of the dinoflagellate genus *Dinophysis*, which contains alloxanthin as a major pigment and shows a cryptomonad-like signature as described before by Meyer-Harms & Pollehne (1998) for the Baltic Sea, and by Schnepf & Elbrächter (1988) and Zapata *et al.* (2012) under laboratory conditions. Several species of *Dinophysis* have been identified in the GHE, reaching densities of almost 1×10^3 cells l^{-1}, and the same densities were also reported for Nervion River Estuary, Spain and Japanese coastal waters (Nishitani *et al.*, 2005; Laza-Martinez *et al.*, 2007). Another possible explanation for this situation might be the existence of relatively large dinoflagellate species in the GHE, such as *Gyrodinium spirale*, reaching densities of almost 1.5×10^3 cells l^{-1}, which also contain high proportions of alloxanthin (Kong *et al.*, 2012). As a consequence, cryptomonad cell counts by microscopic analysis might not match exactly with alloxanthin values, which can show a wider distribution (Gieskes & Kraay, 1983; Rodriguez *et al.*, 2002).

Dense algal blooms, except for a bloom-forming raphidophyte *Heterosigma akashiwo*, were not observed in the GHE during the sampling period. The first bloom of *H. akashiwo* was reported by Tas & Yilmaz (2015) and after that by Dursun *et al.* (2016) almost at the same time in this study area. During this study, a bloom of *H. akashiwo* occured at ST2 in June. In previous studies, the values of major pigments of *H. akashiwo* showed some variations. Generally, the major pigment was found to be fucoxanthin (Jeffrey & Vesk, 1997; Okumura *et al.*, 2012), while others have

additionally reported zeaxanthin and violoxanthin (Fiksdahl *et al.*, 1984; Rodríguez *et al.*, 2006). However, the most abundant pigments were detected as fucoxanthin and chlorophyll-$c_1 + c_2$ for *H. akashiwo* in this study. Also, comparison of pigment values and microscopic cell counts indicates that a significant relationship between fucoxanthin and raphidophyte abundance was observed in the study region (Table 3, N = 42, $P < 0.01$, r = 0.558). Moreover, our results were supported by Butrón *et al.* (2012) for the Bay of Biscay and by Li *et al.* (2003) under culture conditions. As a derivative of fucoxanthin, 19′- butanoyloxyfucoxanthin is presented mainly in chrysophytes (Wright & Jeffrey, 2006; Kong *et al.*, 2012). Exceptionally, a highly significant relationship (Table 3, N = 42, $P < 0.01$, $r = 0.896$) was detected between *H. akashiwo* abundance and 19′- butanoyloxyfucoxanthin in this study period. The highest abundance of *H. akashiwo* was observed at ST2 in June. Moreover, 19′- butanoyloxyfucoxanthin concentrations were only observed in June, when the raphidophytes were dominant in the GHE and maximum concentration ($10.75\,\mu g\,l^{-1}$) was measured at the same time. These findings indicate that 19′-butanoyloxyfucoxanthin might be the main marker pigment, while chlorophyll-$c_1 + c_2$ and fucoxanthin were accessory pigments of *H. akashiwo* in the GHE.

19′-hexanoyloxyfucoxanthin was reported as a major pigment signature of *Emiliania huxleyi*, a bloom-forming prymnesiophyte, by Stolte *et al.* (2000) for all Atlantic strains of this species and by Ediger *et al.* (2006) for the south-western Black Sea. The pigment composition of the chrysophyte, *Apedinella* sp., was characterized by the predominance of 19′-hexanoyloxyfucoxanthin in this study, as reported by Daugbjerg & Henriksen (2001) under laboratory conditions. *Apedinella* sp. appeared only in April and reached maximum abundance at ST1 and ST2. Moreover, 19′-hexanoyloxyfucoxanthin concentrations were commonly observed in April, when chrysophytes were dominant in the GHE and maximum concentration ($0.66\,\mu g\,l^{-1}$) was measured at the same time. A significant relationship (Table 3, N = 42, $P < 0.01$, $r = 0.762$) was detected between *Apedinella* sp. abundance and 19′- hexanoyloxyfucoxanthin.

HPLC pigment analyses and CHEMTAX have been used previously as a valuable monitoring tool in estuaries for determining the absolute or relative contributions of major phytoplankton classes as determined by variations in pigment concentrations (Ansotegui *et al.*, 2001; Paerl *et al.*, 2003; Lewitus *et al.*, 2005). Moreover, there is evidence in the literature that CHEMTAX analysis results were generally consistent with microscopic observations (Wright *et al.*, 1996; Havskum *et al.*, 2004; Llewellyn *et al.*, 2005). However, in recent years, it has been found that one algal species cannot be accurately determined by one specific pigment and different algal groups can share the same pigments, thus affecting the accuracy of the CHEMTAX method (Zapata *et al.*, 2012). There are species that carry 'unambiguous' marker pigments of a different phytoplankton group, e.g. fucoxanthin- and alloxanthin-containing dinoflagellates or only fucoxanthin-containing prymnesiophytes (Jeffrey & Vesk, 1997; Irigoien *et al.*, 2004; Zapata *et al.*, 2004).

An important step to correctly estimate the contribution of different algal classes to chlorophyll-*a* by CHEMTAX is the selection of the appropriate accessory pigment : chlorophyll-*a* ratios (Henriksen *et al.*, 2002; Rodriguez *et al.*, 2002). Therefore, pigment ratios to be used in CHEMTAX should come from the major phytoplankton species native to the area from which the samples were obtained (Mackey *et al.*, 1996; Lewitus *et al.*, 2005). Three different input ratio matrices of pigment : chlorophyll-*a* were tested in this study and matrices were based on pigment ratios published in the literature for oceanic (Matrix 1, Mackey *et al.*, 1996) and estuarine species (Matrix 2, Schlüter *et al.*, 2000 and Matrix 3, Lewitus *et al.*, 2005). As can be seen

in the estimations of Matrix 1, Mackey *et al.*'s (1996) original matrix has required modifications for adapting to different regions – the application of CHEMTAX to estuaries needs to take a typological approach, that is, calibration with species representing the study region. It is not surprising that application of CHEMTAX calibrated with oceanic isolates to estuarine systems can lead to inaccurate predictions of phytoplankton group composition, as originally cautioned by Mackey *et al.* (1996). However, increase or decrease of the initial ratios of pigments of diatoms and dinoflagellates leads to a relatively accurate assessment for diatom composition (Matrix 3) but diatoms still tend to be overestimated. Moreover, CHEMTAX prediction of cryptomonads was also exceptionally poor in all initial ratio matrices (Matrices 1, 2 and 3). This is not surprising, because this group was derived from one species (*Plagioselmis prolonga*) and pigment composition can vary within this class.

In addition to correlations between HPLC pigment analysis and microscopy, phytoplankton classification using CHEMTAX can provide qualitative and quantitative data on the composition of phytoplankton, particularly in complex estuarine ecosystems. Gameiro *et al.* (2007) reported on HPLC derived pigment concentrations and CHEMTAX enabled identification of diatoms, dinoflagellates, cryptomonads, chlorophytes, euglenophytes, prasinophytes, cyanobacteria and haptophytes in the Tagus River estuary, Portugal, and highlighted the reliability of HPLC derived pigment analysis as a tool for the assessment of phytoplankton variability related to community diversity. In this study, it was found that the composition of a phytoplankton community could not be accurately distinguished based on ratio of pigment from the literature, and the calculated results were significantly different from microscopic examination.

The marker pigments detected in this study constitute a high proportion of accessory pigments (fucoxanthin, peridinin, alloxanthin, etc.) and represent, as far as we know, the first detailed description of the distribution patterns of these marker pigments in the Golden Horn Estuary. HPLC derived marker pigments analysis is a useful method for assessment of some phytoplankton groups quantitatively including fragile forms. This method has an advantage over fluorescence microscopy or flow cytometry, where measurements are made on the whole composition from picoplanktonic size to large colonies in a short time. On the other hand, based on the above results, it is suggested that CHEMTAX method cannot accurately characterize the phytoplankton community and needs to be applied carefully to evaluate phytoplankton composition of the Golden Horn Estuary. This indicates that CHEMTAX analysis should always be accompanied by a microscopic analysis due to the ambiguous character of some marker pigments. In future years, combined use of existing methods and also comparison with phytoplankton cell volumes instead of abundances, will be the most reliable way to monitor variations and dynamics of phytoplankton communities. Future investigations, with more frequent sampling periods, including all environmental variables (for example nutrients, light transparency) are needed to establish a clear understanding of HPLC derived phytoplankton pigment signatures in complex estuary ecosystems.

References

Agirbas E, Feyzioglu AM, Kopuz U and Llewellyn CA (2015) Phytoplankton community composition in the south-eastern Black Sea determined with pigments measured by HPLC-CHEMTAX analyses and microscopy cell counts. *Journal of the Marine Biological Association of the United Kingdom* **95**, 35–52.

Agirbas E, Koca L and Aytan U (2017) Spatio-temporal pattern of phytoplankton and pigment composition in surface waters of south-eastern Black Sea. *Oceanologia* **59**, 283–299.

Ansotegui A, Trigueros JM and Orive E (2001) The use of pigment signatures to assess phytoplankton assemblage structure in estuarine waters. *Estuarine, Coastal and Shelf Science* **52**, 689–703.

Ansotegui A, Sarobe A, María Trigueros J, Urrutxurtu I and Orive E (2003) Size distribution of algal pigments and phytoplankton assemblages in a coastal-estuarine environment: contribution of small eukaryotic algae. *Journal of Plankton Research* **25**, 341–355.

Araujoa MLV, Mendesa CRB, Tavanoa VM, Garciaa CAE and Baringerb MO (2017) Contrasting patterns of phytoplankton pigments and chemotaxonomic groups along 30°S in the subtropical South Atlantic Ocean. *Deep-Sea Research I* **120**, 112–121.

Barbosa AB, Domingues RB and Galvão HM (2010) Environmental forcing of phytoplankton in a Mediterranean estuary (Guadiana estuary, southwestern Iberia): a decadal study of anthropogenic and climatic influences. *Estuaries and Coasts* **33**, 324–341.

Barlow RG, Mantoura RFC, Gough MA and Fileman TW (1993) Pigment signatures of the phytoplankton composition in the northeastern Atlantic during the 1990 spring bloom. *Deep Sea Research Part II* **40**, 459–477.

Brunet C and Lizon F (2003) Tidal and diel periodicities of size-fractionated phytoplankton pigment signatures at an offshore station in the southeastern English Channel. *Estuarine Coastal and Shelf Science* **56**, 833–843.

Burić Z, Cetinić I, Viličić D, Mihalić KC, Carić M and Olujić G (2007) Spatial and temporal distribution of phytoplankton in a highly stratified estuary (Zrmanja, Adriatic Sea). *Marine Ecology* **28**, 169–177.

Butrón A, Madariaga I and Orive E (2012) Tolerance to high irradiance levels as a determinant of the bloom-forming *Heterosigma akashiwo* success in estuarine waters in summer. *Estuarine Coastal and Shelf Science* **107**, 141–149.

Campbell L and Vaulot D (1993) Photosynthetic picoplankton community structure in the subtropical North Pacific Ocean near Hawaii (station ALOHA). *Deep-Sea Research I* **40**, 2043–2060.

Carreto JI, Montoya NG, Benavides HR, Guerrero R and Carignan MO (2003) Characterization of spring phytoplankton communities in the Río de La Plata maritime front using pigment signatures and cell microscopy. *Marine Biology* **143**, 1013–1027.

Daugbjerg N and Henriksen P (2001) Pigment composition and rbcL sequence data from the silicoflagellate *Dictyocha speculum*: a heterokont alga with pigments similar to some haptophytes. *Journal of Phycology* **37**, 1110–1120.

Dursun F and Tas S (2019) Variations in abundance and diversity of phytoplankton in the surface waters of the Golden Horn Estuary (Sea of Marmara). *Journal of the Marine Biological Association of the United Kingdom* **99**, 279–290.

Dursun F, Taş S and Koray T (2016) Spring bloom of the raphidophycean *Heterosigma akashiwo* in the Golden Horn Estuary at the northeast of Sea of Marmara. *Ege Journal of Fisheries and Aquatic Sciences* **33**, 201–207.

Ediger D, Soydemir N and Kideys AE (2006) Estimation of phytoplankton biomass using HPLC pigment analysis in the southwestern Black Sea. *Deep Sea Research Part II: Topical Studies in Oceanography* **53**, 1911–1922.

Eker-Develi E, Berthon JF and Linde D (2008) Phytoplankton class determination by microscopic and HPLC-CHEMTAX analyses in the southern Baltic Sea. *Marine Ecology Progress Series* **359**, 69–87.

Eker-Develi E, Berthon JF, Canuti E, Slabakova N, Moncheva S, Shtereva G and Dzhurova B (2012) Phytoplankton taxonomy based on CHEMTAX and microscopy in the northwestern Black Sea. *Journal of Marine Systems* **94**, 18–32.

Everitt DA, Wright SW, Volkman JK, Thomas DP and Lindstrom EJ (1990) Phytoplankton community compositions in the western equatorial Pacific determined from chlorophyll and carotenoid pigment distributions. *Deep-Sea Research I* **37**, 975–997.

Fiksdahl A, Withers N and Liaaen-Jensen S (1984) Carotenoids of *Heterosigma akashiwo*: a chemosystematic contribution. *Biochemical Systematics and Ecology* **12**, 355–356.

Gameiro C, Cartaxana P and Brotas V (2007) Environmental drivers of phytoplankton distribution and composition in Tagus Estuary, Portugal. *Estuarine, Coastal and Shelf Science* **75**, 21–34.

Garibotti IA, Vernet M, Kozlowski WA and Ferrario ME (2003) Composition and biomass of phytoplankton assemblages in coastal Antarctic waters: a comparison of chemotaxonomic and microscopic analyses. *Marine Ecology Progress Series* **247**, 27–42.

Gibb SW, Barlow RG, Cummings DG, Rees NW, Trees CC, Holligan P and Suggett D (2000) Surface phytoplankton pigment distributions in the Atlantic Ocean: an assessment of basin scale variability between 50 N and 50 S. *Progress in Oceanography* **45**, 339–368.

Gieskes WWC and Kraay GW (1983) Dominance of Cryptophyceae during the phytoplankton spring bloom in the central North Sea detected by HPLC analysis of pigments. *Marine Biology* **75**, 179–185.

Havskum H, Schlüter L, Scharek R, Berdalet E and Jacquet S (2004) Routine quantification of phytoplankton groups – microscopy or pigment analyses? *Marine Ecology Progress Series* **273**, 31–42.

Henriksen P, Riemann B, Kaas H, Sørensen HM and Sørensen HL (2002) Effects of nutrient-limitation and irradiance on marine phytoplankton pigments. *Journal of Plankton Research* **24**, 835–858.

Higgins HW, Wright SW and Schlüter L (2011) Quantitative interpretation of chemotaxonomic pigment data. In Roy S, Llewellyn CA, Egeland ES and Johnson G (eds), *Phytoplankton Pigments: Characterization, Chemotaxonomy and Applications in Oceanography*. Cambridge: Cambridge University Press, pp. 257–313.

Hillebrand H, Dürselen CD, Kirschtel D, Pollingher U and Zohary T (1999) Biovolume calculation for pelagic and benthic microalgae. *Journal of Phycology* **35**, 403–424.

Irigoien X, Meyer B, Harris R and Harbour D (2004) Using HPLC pigment analysis to investigate phytoplankton taxonomy: the importance of knowing your species. *Helgoland Marine Research* **58**, 77–82.

Islabão CA, Mendes CRB, Russo ADPG and Odebrecht C (2016) Effects of irradiance on growth, pigment content and photosynthetic efficiency on three peridinin-containing dinoflagellates. *Journal of Experimental Marine Biology and Ecology* **485**, 73–82.

Jasprica N, Carić M, Kršinić F, Kapetanović T, Batistić M and Njire J (2012) Planktonic diatoms and their environment in the lower Neretva River estuary. *Nova Hedwigia Beihefte* **141**, 405–430.

Jeffrey SW and Vesk M (1997) Introduction to marine phytoplankton and their pigment signatures. In Jeffrey SW, Mantoura RFC and Wright SW (eds), *Phytoplankton Pigments in Oceanography: Guidelines to Modern Methods. Monographs on Oceanographic Methodology*, 10. Paris: UNESCO, pp. 37–84.

Kong F, Yu R, Zhang Q, Yan T and Zhou M (2012) Pigment characterization for the 2011 bloom in Qinhuangdao implicated "brown tide" events in China. *Chinese Journal of Oceanology and Limnology* **30**, 361–370.

Kozlowski WA, Deutschman D, Garibotti I, Trees C and Vernet M (2011) An evaluation of the application of CHEMTAX to Antarctic coastal pigment data. *Deep-Sea Research I* **58**, 350–364.

Krivokapić S, Bosak S, Viličić D, Kušpilić G, Drakulović D and Pestorić B (2018) Algal pigments distribution and phytoplankton group assemblages in coastal transitional environment – Boka Kotorska Bay (South eastern Adriatic Sea). *Acta Adriatica* **59**, 35–50.

Latasa M (2007) Improving estimations of phytoplankton class abundances using CHEMTAX. *Marine Ecology Progress Series* **329**, 13–21.

Laza-Martinez A, Seoane S, Zapata M and Orive E (2007) Phytoplankton pigment patterns in a temperate estuary: from unialgal cultures to natural assemblages. *Journal of Plankton Research* **29**, 913–929.

Lewitus AJ, White DL, Tymowski RG, Geesey ME, Hymel SN and Noble PA (2005) Adapting the CHEMTAX method for assessing phytoplankton taxonomic composition in Southeastern U.S. estuaries. *Estuaries* **28**, 160–172.

Li D, Cong W, Cai Z, Shi D and Ouyang F (2003) Some physiological and biochemical changes in marine eukaryotic red tide alga *Heterosigma akashiwo* during the alleviation from iron limitation. *Plant Physiology and Biochemistry* **41**, 295–301.

Lionard M, Muylaert K, Tackx M and Vyverman W (2008) Evaluation of the performance of HPLC-CHEMTAX analysis for determining phytoplankton biomass and composition in a turbid estuary (Schelde, Belgium). *Estuarine, Coastal and Shelf Science* **76**, 809–817.

Llewellyn C, Fishwick JR and Blackford JC (2005) Phytoplankton community assemblage in the English Channel: a comparison using chlorophyll

a derived from HPLC-CHEMTAX and carbon derived from microscopy cell counts. *Journal of Plankton Research* 27, 103–119.

Mackey MD, Mackey DJ, Higgins HW and Wright SW (1996) CHEMTAX – a program for estimating class abundances from chemical markers: application to HPLC measurements of phytoplankton. *Marine Ecology Progress Series* 144, 265–283.

Mantoura RFC and Llewellyn CA (1983) The rapid determination of algal chlorophyll and carotenoid pigments and their breakdown products in natural waters by reverse-phase high-performance liquid chromatography. *Analytica Chimica Acta* 151, 297–314.

Meyer-Harms B and Pollehne F (1998) Alloxanthin in *Dinophysis norvegica* (Dinophysiales, Dinophyceae) from the Baltic Sea. *Journal of Phycology* 34, 280–285.

Millie DF, Paerl HW and Hurley JP (1993) Microalgal pigment assessments using high-performance liquid chromatography: a synopsis of organismal and ecological applications. *Canadian Journal of Fisheries and Aquatic Sciences* 50, 2513–2527.

Naik RK, Anil AC, Narale DD, Chitari RR and Kulkarni VV (2011) Primary description of surface water phytoplankton pigment patterns in the Bay of Bengal. *Journal of Sea Research* 65, 435–441.

Nishitani G, Yamaguchi M, Ishikawa A, Yanagiya S, Mitsuya T and Imai I (2005) Relationships between occurrences of toxic *Dinophysis* species (Dinophyceae) and small phytoplanktons in Japanese coastal waters. *Harmful Algae* 4, 755–762.

Okumura Y, Yamasaki M, Suzuki T, Ichimi K and Oku O (2012) Pigment profile and violaxanthin cycle of *Heterosigma akashiwo*. *Journal of Shellfish Research* 20, 1263–1268.

Olson RJ, Chisholm SW, Zettler ER, Altabet MA and Dusenberry JA (1990) Spatial and temporal distributions of prochlorophyte picoplankton in the north Alantic Ocean. *Deep-Sea Research* 37, 1033–1051.

Paerl HW, Valdes LM, Pinckney JL, Piehler MF, Dyble J and Moisander PH (2003) Phytoplankton photopigments as indicators of estuarine and coastal eutrophication. *BioScience* 53, 953–964.

Pérez V, Fernández E, Marañón E, Morán XAG and Zubkov MV (2006) Vertical distribution of phytoplankton biomass, production and growth in the Atlantic subtropical gyres. *Deep Sea Research Part I: Oceanographic Research Papers* 53, 1616–1634.

Rodriguez F, Varela M and Zapata M (2002) Phytoplankton assemblages in the Gerlache and Bransfield Straits (Antarctic Peninsula) determined by light microscopy and CHEMTAX analysis of HPLC pigment data. *Deep Sea Research Part II: Topical Studies in Oceanography* 49, 723–747.

Rodríguez F, Chauton M, Johnsen G, Andresen K, Olsen LM and Zapata M (2006) Photoacclimation in phytoplankton: implications for biomass estimates, pigment functionality and chemotaxonomy. *Marine Biology* 148, 963–971.

Schlüter L, Mohlenberg F, Havskum H and Larsen S (2000) The use of phytoplankton pigments for identifying and quantifying phytoplankton groups in coastal areas: testing the influence of light and nutrients on pigment/chlorophyll a ratios. *Marine Ecology Progress Series* 192, 49–63.

Schnepf E and Elbrächter M (1988) Cryptophycean-like double membrane-bound chloroplast in the dinoflagellate, *Dinophysis* Ehrenb.: evolutionary, phylogenetic and toxicological implications. *Botanica Acta* 101, 196–203.

Seoane S, Laza A and Orive E (2006) Monitoring phytoplankton assemblages in estuarine waters: the application of pigment analysis and microscopy to size-fractionated samples. *Estuarine Coastal and Shelf Science* 67, 343–354.

Seoane S, Garmendia M, Revilla M, Borja Á, Franco J, Orive E and Valencia V (2011) Phytoplankton pigments and epifluorescence microscopy as tools for ecological status assessment in coastal and estuarine waters, within the Water Framework Directive. *Marine Pollution Bulletin* 62, 1484–1497.

Silva A, Mendes CR, Palma S and Brotas V (2008) Short-time scale variation of phytoplankton succession in Lisbon Bay (Portugal) as revealed by microscopy cell counts and HPLC pigment analysis. *Estuarine Coastal and Shelf Science* 79, 230–238.

Smith VH, Tilman GD and Nekola JC (1999) Eutrophication: impacts of excess nutrient inputs on freshwater, marine, and terrestrial ecosystems. *Environmental Pollution* 100, 179–196.

Stolte W, Kraay GW, Noordeloos AAM and Riegman R (2000) Genetic and physiological variation in pigment composition of *Emiliania huxleyi* (Prymnesiophyceae) and the potential use of its pigment ratios as a quantitative physiological marker. *Journal of Phycology* 36, 529–539.

Sur HI, Okuş E, Sarikaya HZ, Altiok H, Eroğlu V and Öztürk I (2002) Rehabilitation and water quality monitoring in the Golden Horn. *Water Science and Technology* 46, 29–36.

Tas S (2015) A prolonged red tide of *Heterocapsa triquetra* (Ehrenberg) F. Stein (Dinophyceae) and phytoplankton succession in a eutrophic estuary (Turkey). *Mediterranean Marine Science* 16, 621–627.

Tas S (2017) Planktonic diatom composition and environmental conditions in the Golden Horn Estuary (Sea of Marmara, Turkey). *Fundamental and Applied Limnology* 189, 153–166.

Tas S (2019) Microalgal blooms in a eutrophic estuary (Golden Horn, Sea of Marmara) following a remediation effort. *Botanica Marina* 62, 537–547.

Tas S and Okus E (2011) A review on the bloom dynamics of a harmful dinoflagellate *Prorocentrum minimum* in the Golden Horn Estuary. *Turkish Journal of Fisheries and Aquatic Sciences* 11, 673–681.

Tas S and Yilmaz IN (2015) Potentially harmful microalgae and algal blooms in a eutrophic estuary in the Sea of Marmara (Turkey). *Mediterranean Marine Science* 16, 432–443.

Tas S and Hernández-Becerril DU (2017) Diversity and distribution of the planktonic diatom genus Chaetoceros (Bacillariophyceae) in the Golden Horn Estuary (Sea of Marmara). *Diatom Research* 32, 309–323.

Tas S and Lundholm N (2017) Temporal and spatial variability of the potentially toxic *Pseudo-nitzschia* spp. in a eutrophic estuary (Sea of Marmara). *Journal of the Marine Biological Association of the United Kingdom* 97, 1483–1494.

Tas S, Yilmaz IN and Okus E (2009) Phytoplankton as an indicator of improving water quality in the Golden Horn Estuary. *Estuaries and Coasts* 32, 1205–1224.

Tas S, Dursun F, Aksu A and Balkis N (2016) Presence of the diatom genus *Pseudo-nitzschia* and particulate domoic acid in the Golden Horn Estuary (Sea of Marmara, Turkey). *Diatom Research* 31, 339–349.

Throndsen NJ (1978) Preservation and storage. In Sournia A (ed.), *Phytoplankton Manual*. Paris: UNESCO, pp. 69–74.

Thyssen M, Beker B, Ediger D, Yilmaz D, Garcia N and Denis M (2011) Phytoplankton distribution during two contrasted summers in a Mediterranean harbour: combining automated submersible flow cytometry with conventional techniques. *Environmental Monitoring and Assesment* 173, 1–16.

Totti C (2000) Seasonal variability of phytoplankton populations in the middle Adriatic sub-basin. *Journal of Plankton Research* 22, 1735–1756.

Trigueros JM and Orive E (2001) Seasonal variations of diatoms and dinoflagellates in a shallow, temperate estuary, with emphasis on neritic assemblages. *Hydrobiologia* 444, 119–133.

Ünlülata Ü, Oğuz T, Latif MA and Özsoy E (1990) On the physical oceanography of the Turkish Straits. In Pratt LJ (ed.), *The Physical Oceanography of Sea Straits*. Cham: Springer, pp. 25–60.

Utermöhl H (1958) Zur vervollkommnung der quantitativen phytoplanktonmethodik. *Limnologie: Mitteilungen* 9, 1–38.

Veldhuis MJW and Kraay GW (1990) Vertical distribution and pigment composition of a picoplanktonic prochlorophyte in the subtropical north Atlantic: a combined study of HPLC analysis of pigments and flow cytometry. *Marine Ecology Progress Series* 68, 121–127.

Veldhuis MJW and Kraay GW (2000) Application of flow cytometry in marine phytoplankton research: current applications and future perspectives. *Scientia Marina* 64, 121–134.

Veldhuis MJ and Kraay GW (2004) Phytoplankton in the subtropical Atlantic Ocean: towards a better assessment of biomass and composition. *Deep Sea Research Part I: Oceanographic Research Papers* 51, 507–530.

Wänstrand I and Snoeijs P (2006) Phytoplankton community dynamics assessed by ships-of-opportunity sampling in the northern Baltic Sea: a comparison of HPLC pigment analysis and cell counts. *Estuarine Coastal and Shelf Science* 66, 135–146.

Wong CK and Wong CK (2009) Characteristics of phytoplankton community structure during and after a bloom of the dinoflagellate *Scrippsiella trochoidea* by HPLC pigment analysis. *Journal of Ocean University of China* 8, 141–149.

Wright SW and Jeffrey SW (2006) Pigment markers for phytoplankton production. In Volkman JK (ed.), *Marine Organic Matter: Biomarkers, Isotopes and DNA*. Berlin: Springer, pp. 71–104.

Wright SW, Thomas DP, Marchant HJ, Higgins HW, Mackey MD and Mackey DJ (1996) Analysis of phytoplankton of the Australian sector of the Southern Ocean: comparisons of microscopy and size frequency data with interpretations of pigment HPLC data using the 'CHEMTAX' matrix factorisation program. *Marine Ecology Progress Series* 144, 285–298.

Yücel N (2017) Variability in phytoplankton pigment composition in Mersin Bay. *Turkish Journal of Fisheries and Aquatic Sciences* **32**, 49–70.

Zapata M, Jeffrey SW, Wright SW, Rodríguez F, Garrido JL and Clementson L (2004) Photosynthetic pigments in 37 species (65 strains) of Haptophyta: implications for oceanography and chemotaxonomy. *Marine Ecology Progress Series* **270**, 83–102.

Zapata M, Fraga S, Rodríguez F and Garrido JL (2012) Pigment-based chloroplast types in dinoflagellates. *Marine Ecology Progress Series* **465**, 33–52.

Zhang Z, Green BR and Cavalier-Smith T (2000) Phylogeny of ultra-rapidly evolving dinoflagellate chloroplast genes: a possible common origin for sporozoan and dinoflagellate plastids. *Journal of Molecular Evolution* **51**, 26–40.